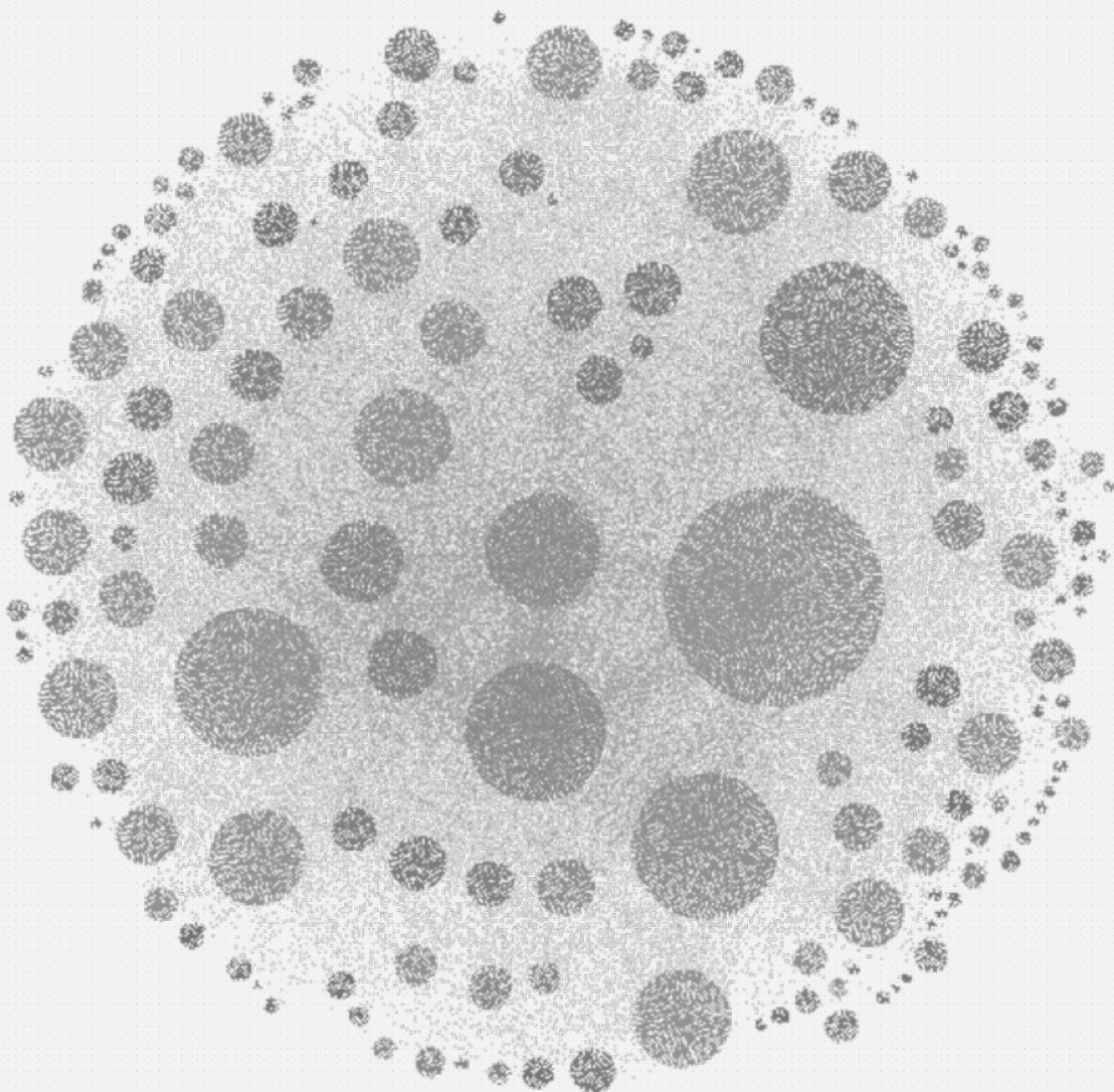


Support Vector Machines

Bruno Vandekerkhove



In this document each exercise session is dealt with in separate sections that are named correspondingly.

Contents

Classification	1
Two Gaussians	1
Support Vector Machine Classifier	1
Least-squares support vector machine classifier	3
Ripley dataset	5
Wisconsin breast cancer dataset	6
Diabetes dataset	7
Function Estimation and Time Series Prediction	8
Support vector machine for function estimation	8
A simple example: the sinc function	8
Automatic Relevance Determination	10
Robust regression	10
Logmap dataset	11
Santa Fe dataset	12
Unsupervised Learning and Large Scale Problems	13
Kernel principal component analysis	13
Spectral clustering	14
Fixed-size LS-SVM	15
Kernel principal component analysis	16
Fixed-size LS-SVM	16

Classification

/src/session_1.m, /src/homework_1.m

Two Gaussians

For a binary classifier where the distributions are (assumed or known to be) Gaussian with equal covariance matrices the decision boundary that maximises the posterior probability $P(C_i|x)$ becomes linear. This is independent of the amount of overlap. Trying to get a better boundary would lead to overfitting. In this particular example where $\Sigma_{xx} = \mathbb{I}$ one ends up with a perpendicular bisector of the segment connecting the two cluster means $(-1, -1)$ and $(1, 1)$, which gives $f(x) = -x$ as a decision boundary.

Support Vector Machine Classifier

To deal with the non-linearly separable classification problem in the example one solves the following minimisation problem, where the hyperparameter C controls the tradeoff between maximising the margin and making sure that the data lies on the correct side of that margin :

$$\min_w \frac{1}{2} \cdot w^T \cdot w + C \cdot \sum_{k=1}^N \xi_k \quad \text{such that } y_k \cdot [w^T \cdot x_k + b] \geq 1 - \xi_k \text{ and } \xi_k \geq 0 \ (\forall k \in \{1, \dots, N\})$$

A dual form can be expressed by making use of Lagrange multipliers which in this context are also called *support values*. Any data points for which the corresponding support value isn't zero are called *support vectors*. These lie close to the boundary or are misclassified¹.

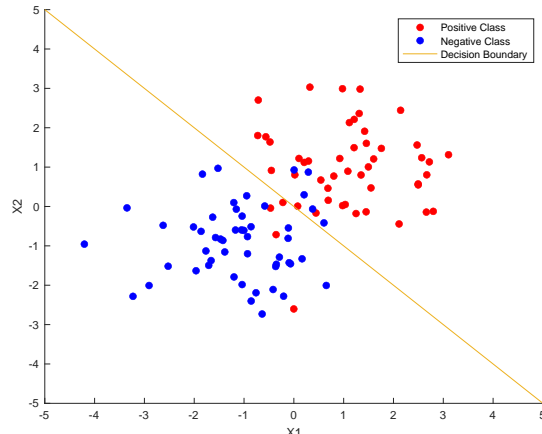


Figure 1: Decision boundary (in orange) for two Gaussian distributions with equal covariance matrices.

¹In the dual problem formulation the α values are minimised for those data points that are ‘similar’ to data points that belong to the same class.

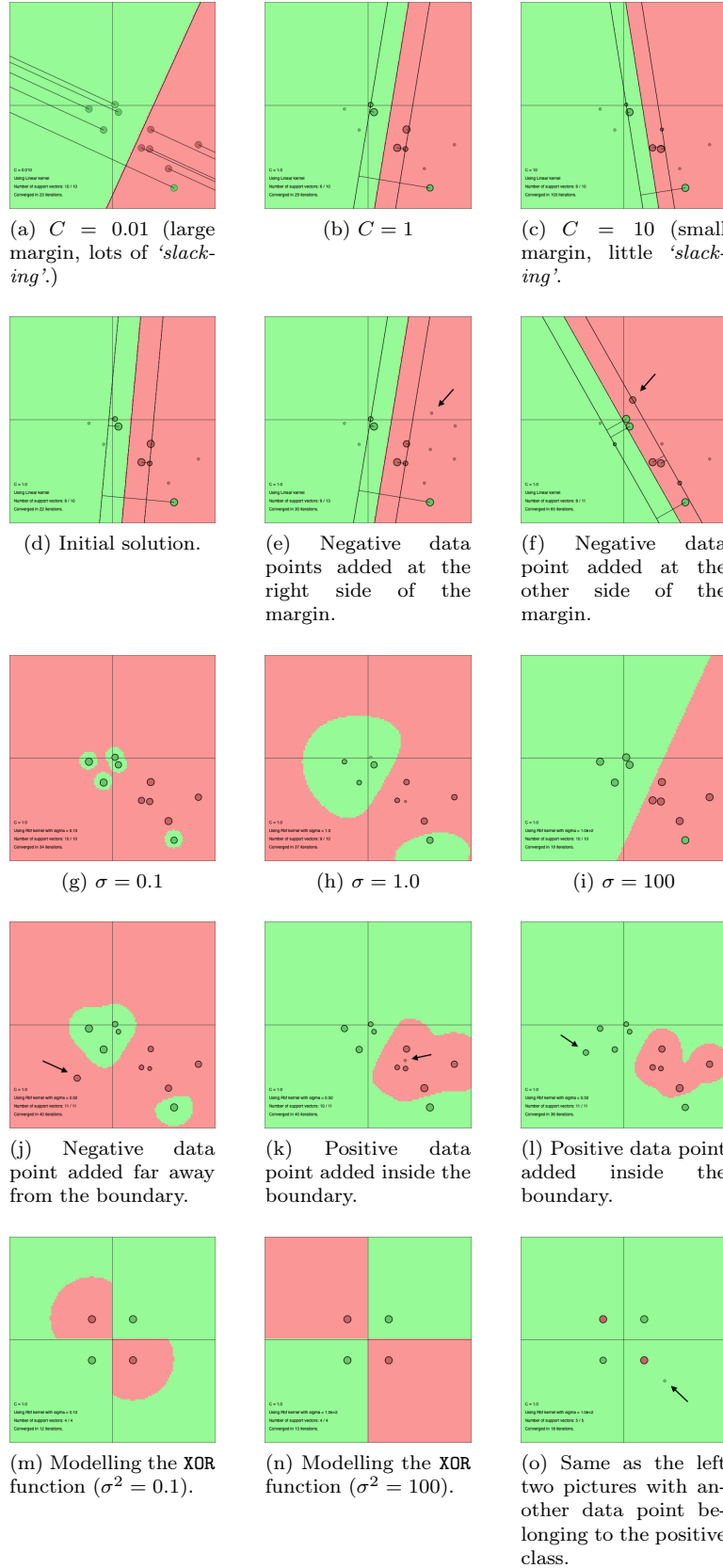


Figure 2: Visualisation of various experiments with C (top row), addition of points using the linear kernel (second row), σ (third row), addition of points using the RBF kernel (fourth row) and the XOR function (last row). The number of iterations (tends to) increase as C gets larger or as the number of data points increases.

For the given toy dataset it can readily be seen in figure 2 (top row) that for a decreasing value of C the margin does become larger and that less ‘slackening’ is allowed for. By adding data points close to the boundary or at the ‘wrong’ side of it the margin usually changes a lot and the new data points nearly always become support vectors.

The σ^2 hyperparameter in the case of an RBF kernel controls the locality of each data point. As it increases the feature space mapping becomes smoother, producing simpler decision boundaries (figure 2, third row). This relates to the bias-variance tradeoff. For σ^2 small enough any two classes get separated in a very strict way - the Gaussian kernels are universal. In the limit the kernel matrix becomes an identity matrix. For large bandwidths the reach of each data point becomes large and the decision boundary can become near-linear as the density areas of each class end up competing². In the limit the kernel matrix is filled with ones and the classification fails (in the demo this can happen at $\sigma^2 = 10^5$, in the LS-SVM toolbox a much larger value is needed). As for C , it works the same as before, prioritising either larger margins or lower misclassification rates. When σ^2 is large a bigger value of C can make the model more complex again.

The RBF kernel approach can generate models having misclassification rates that are lower than the classic linear kernel approach does as decision boundaries that are nonlinear in the input space can be learned. It also tends to use more data points as support vectors. This makes the model less compact (computationally efficient) and if the data is linearly separable it is unnecessary. Deciding whether the model generalises better can be done through evaluation on a test set.

Least-squares support vector machine classifier

Figure 3 depicts results on the iris dataset using various polynomial kernels with $t = 1$. This t is called the *constant* and it controls the importance of higher - versus lower-order terms in the polynomial as can be deduced from the application of the binomial theorem to the definition of the kernel :

$$(x^T \cdot y + \tau)^d = \sum_{i=0}^d \binom{d}{i} (x^T \cdot y)^{d-i} \cdot \tau^i$$

The effect of t is not very noticeable for small values of d while for the higher degrees it tends to make the decision boundary more complex.

When the degree δ is 1 the feature map is linear which is equivalent to the classic non-linear SVM problem while for higher degrees a boundary of increasing complexity is learned such that for $\delta \in \{3, 4\}$ no data points are misclassified. To make it less likely that the model overfits a lower δ is likely to be preferable (this corresponds to the application of Occam’s razor).

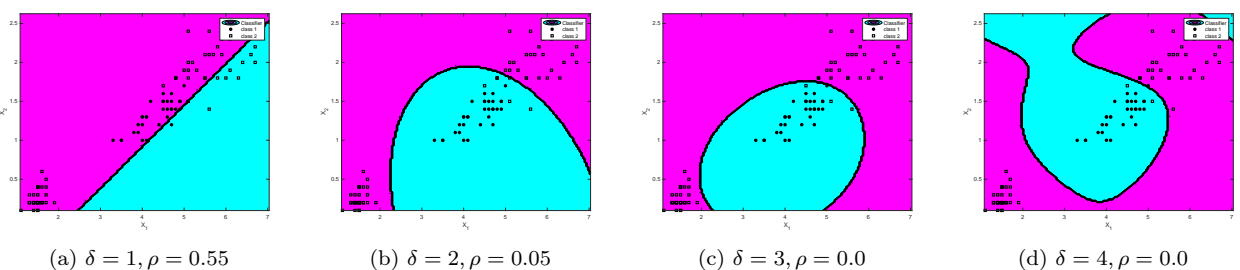


Figure 3: Visualisation of the results of experiments with polynomial kernels on the iris dataset (δ is the degree of the polynomial, ρ the misclassification rate on the test set, t is fixed to 1). As the degree of the kernel increases, the misclassification error drops.

In the case of RBF kernels one can see in figure 4 that for a γ value of 1 any σ^2 between 0.1 and 1 performs well. The same interval works for γ when $\sigma^2 = 1$. This corresponds to the results of the provided sample script where the base used in the semilog plot happens to be the natural logarithm (instead of using base 10). For large σ values (say, 25) one class may overtake the other one. The experiment is of limited value as only few parameter combinations were tried.

To properly find good parameter values a more systematic approach is in order. The idea is to search through the parameter space and evaluate the results on a validation set rather than on the test set (which should be

²When the demo is run on a 4-point dataset representing the `XOR` function a checkerboard pattern is obtained when σ^2 is large (as seen in figure 2, last row). Even when σ^2 is low the separation is linear in between the data points as the problem reduces to that seen in the introductory example.

used for nothing but the evaluation of the finished model). A validation set can be constructed in a few ways the results of which are illustrated in figure 6, where error estimates in the parameter space are shown. Random splitting i.e. splitting the input data randomly in a training - and a validation set is a way that isn't particularly robust. An improvement upon it is k -fold validation where the input data is randomly split into k folds which are considered as a validation set in turn such that all the input data can be used for parameter tuning. When $k = N$ with N the number of input samples this is called leave-one-out cross-validation.

To some extent deciding what k value to use parallels previous discussions about other parameters since there's a bias-variance tradeoff ; while larger k values should provide a better estimate of the error they also suffer from higher variance as the result depends more on how representative the input data is. This becomes more important when the number of input data is small. Finally, k shouldn't be too small (such that the training sets remain large enough), it should preferably be a divisor of N (though this is not of primary importance) and if computational expense is an issue it cannot be large as many models would have to be generated (which admittedly can be addressed).

Automated tuning uses these validation methods in conjunction with a search procedure to find useful combinations of parameters. This search strategy has to deal with a non-convex problem and can be a simple grid search (performing validation for every combination of parameters specified by a grid partitioning the parameter space) or the Nelder-Mead method. The latter aims to find the minimum of a function without needing its derivative by considering a simplex which is updated iteratively until it wraps around the minimum. It tends to execute faster than grid search especially when the number of parameters is high, though to address this one could also consider a variant of grid search that starts with a grid of limited granularity until it finds a promising region in the parameter space on which grid search is performed again.

In the LS-SVM toolbox a technique called *coupled simulated annealing* is used. This is a global optimisation technique which couples together several simulated annealing processes (inspired by coupled local minimisers' effectiveness compared to multi-start gradient descent optimisation). Its output is subsequently provided to either a grid search - or a Nelder-Mead algorithm. Results are the following :

<i>Method</i>	γ	σ^2	<i>cost</i>
Grid search	$16983.8488 \pm 100324.6730$	10.5373 ± 83.0560	0.0339 ± 0.0063
Nelder-Mead	$85111.5137 \pm 75855.5677$	12.8189 ± 71.4858	0.0349 ± 0.0069

Table 1: Results of automated tuning strategies (averaged over 100 runs).

Simulated annealing is a stochastic process such that the parameters end up varying quite a bit. The costs do not since they are minimised. A histogram of the results gives a more complete picture and shows that there are a few outliers that make the average γ and σ^2 large :

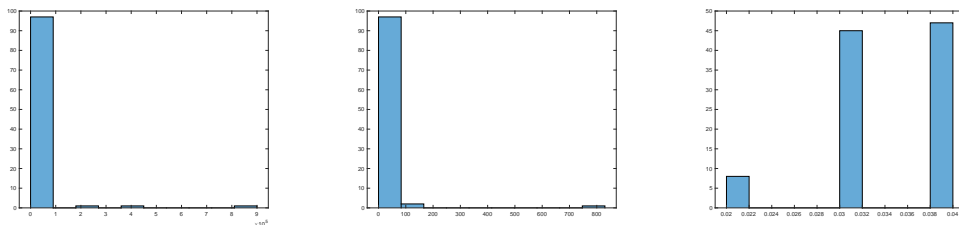


Figure 5: Histograms for 100γ , σ^2 and costs returned by the automated tuning process.

Results of the automated tuning process correspond to the contour plots given in figure 6. As for the runtimes, the grid search ended up being twice as slow as the simplex method.

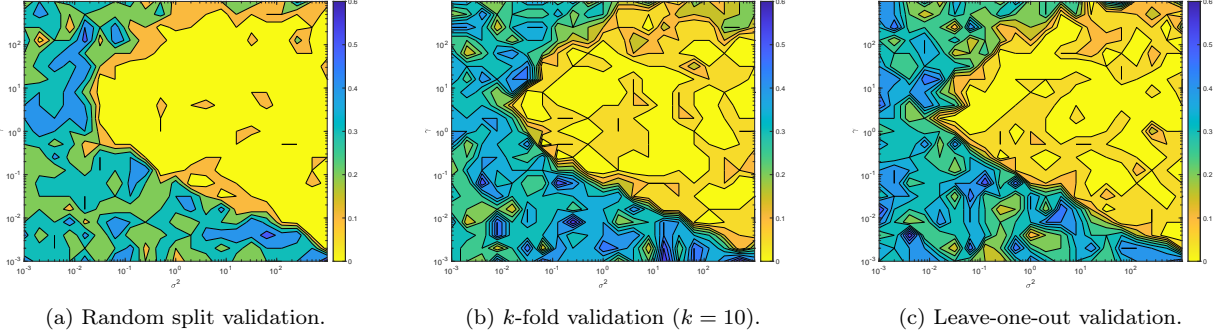


Figure 6: Grid search in conjunction with various validation techniques. The results differ and the results for the random split strategy varies between runs. k -fold crossvalidation appears to be a better approximation of the error but may generalise less well. Reasonable parameters lie in the yellow zone where the error reaches a maximum of about 10%. A small bandwidth of between say, 0.1 and 1.0 and a regularization constant of 1.0 seems reasonable.

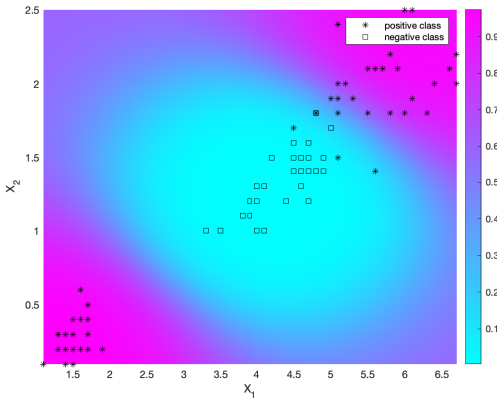


Figure 7: Posterior probability estimates using a Bayesian approach ($\gamma \approx 0.038, \sigma^2 \approx 0.56$). The hue indicates the probability that the data point at a location in the 2-dimensional plane belongs to one or the other class. A smaller σ^2 can lead to overfitting and makes for a more clearly defined, smaller blue area.

An ROC curve can be generated for any model. One calculates the result of the model applied on every test data point and uses the results as thresholds for which the true positive rate (TPR) is plotted in function of the false positive rate (FPR). The area under the curve (AUC) can then be used to gauge the effectiveness of the classifier. For $\gamma = 0.037622, \sigma^2 = 0.559597$ it happens to equal 1 indicating a perfect classifier. If the `sign` function had been used to classify test data there would be a misclassification error (the FPR would be 0.1).

Using a Bayesian approach (considered in greater detail in the second part of this report) which requires a prior denoting the probability of occurrence of each class it is possible (by applying Bayes' theorem) to estimate the probability that a given data point belongs to the positive or the negative class. A corresponding plot of these posterior probabilities for the same model used to calculate the ROC curve is shown in figure 7. The prior is taken to be 0.67 (the classes are unbalanced).

Ripley dataset

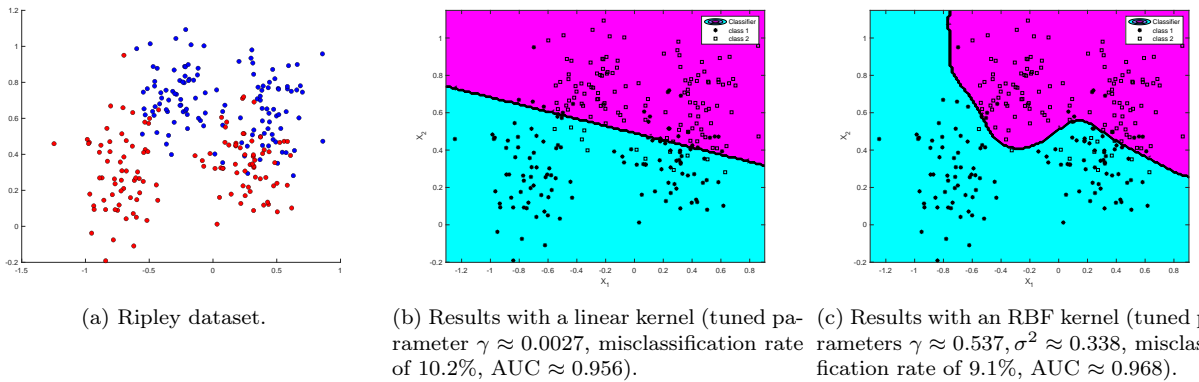


Figure 8: The Ripley dataset and results with a linear and an RBF kernel. LSSVMs are used. The number of support vectors equals 250 (100%) in all cases.

The Ripley dataset is a 2-dimensional so it can easily be visualised (figure 8). The data for each class is generated by a mixture of two Gaussian distributions and it is not linearly separable in the input space. The distributions were chosen as to ‘allow a best-possible error rate of about 8%’, each component has the same covariance matrix

(basically a 2-component version of the introductory example). The data is a ‘*realistic*’ toy problem and it is rather noisy.

An LS-SVM with a linear kernel makes for a classification rate of around 10% while an RBF kernel performs a tad better at a rate of about 9% (and so does a polynomial one³). The ROC curves give a more complete picture and aren’t shown here, but the AUC was the highest for the RBF kernel (about 0.97) with accuracy being the highest at a threshold a bit below zero. In practice (when met with real-life datasets) operating points on the ROC curve calculated on the validation set may be chosen depending on the cost of each type of misclassification.

Steve Gunn’s MATLAB toolbox which is also used for regression in the second part of the report provides functions for generating classical SVMs and some more kernels that can be experimented with though it provides no automated tuning method for these. The results for linear -, RBF and polynomial kernels are about the same though there are less support vectors. Results after manual tuning (through the `uiclass` interface) are shown in figure 9.

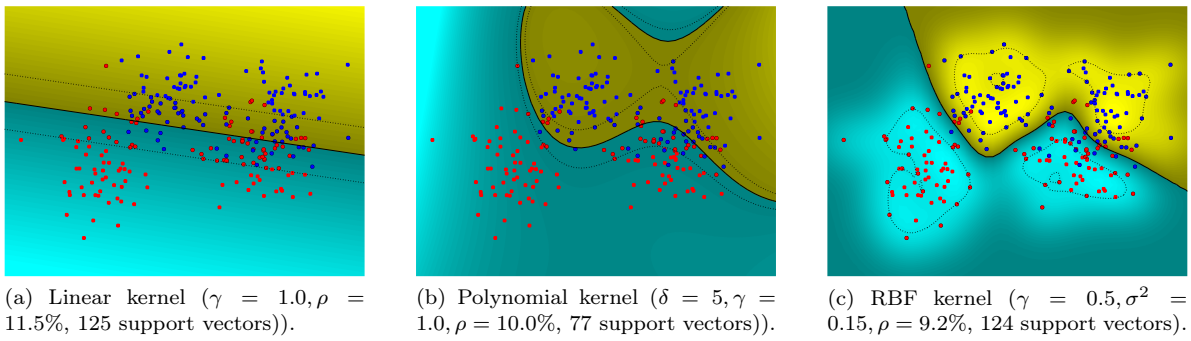


Figure 9: The Ripley dataset and results with a linear and an RBF kernel. LSSVMs are used.

Since the dataset is Gaussian an RBF kernel should be an appropriate pick. As it’s also a noisy dataset a smoother decision surface (higher σ^2 and/or lower γ) should be opted for. Of course in this case the optimal classifier (in terms of maximisation of the posterior probabilities) can be defined based on Bayes’ theorem.

Wisconsin breast cancer dataset

With 30 features for each of the observations the Wisconsin breast cancer diagnosis dataset isn’t trivial to visualise. MATLAB has an implementation of t-SNE or two principal components determined through PCA could be plotted (see figure 11). Distributions of some of the features are shown below. The two classes denote benign - or malignant cancer tissue. In contrast with the previous dataset this one’s a bit unbalanced (62.5% belongs to the negative class) which can be accounted for through bias correction⁴ or by using weights in the SVM formulation to give more emphasis to the terms associated to the minority class.

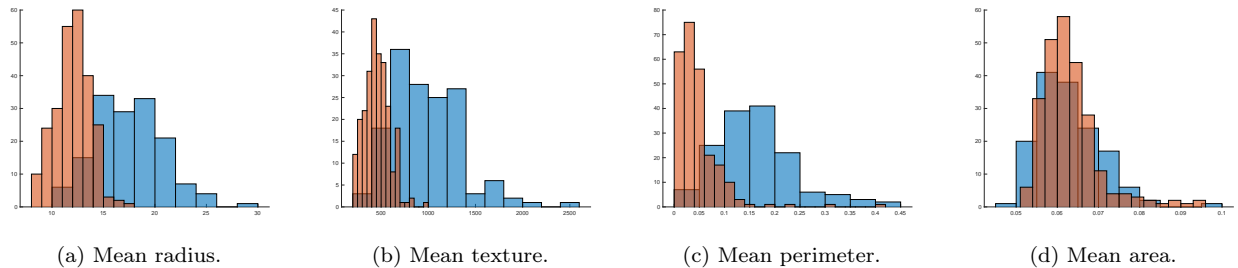


Figure 10: Distributions of the first 4 features of the Wisconsin breast cancer dataset (red denotes malignant -, blue denotes benign tumors). There are 10 features in total and for each of these the mean, standard error and maximum value is given. For some of the features none of those three appear to be particularly informative.

A simple automated tuning experiment of an LS-SVM with linear -, polynomial - and RBF kernels yielded average AUCs of 0.996 ± 0.001 , 0.937 ± 0.058 and 0.995 ± 0.002 respectively. It may be surprising that a linear

³Automated tuning of the polynomial usually resulted in a degree δ between 4 and 7.

⁴Whilst doing so it came to my attention that the `roc` function in the LS-SVM toolbox *seems* to return the thresholds in the wrong (reverse) order.

	ARD (RBF kernel)	PCA ($n_h = 2$)	PCA ($n_h = 3$)	PCA ($n_h = 10$)
Error	$2.075\% \pm 0.206$	$6.125\% \pm 0.339$	$3.825\% \pm 0.237$	$3.750\% \pm 0.167$
AUC	0.99723 ± 0.00040	0.98402 ± 0.00335	0.99077 ± 0.00238	0.98729 ± 0.00520

Table 2: Mean and standard deviation of accuracy and AUC for linear kernel models after application of two types of dimensionality reduction ; PCA or automatic relevance determination (which selected 21 features). PCA was applied by subtracting the mean, applying PCA on the training set and using the resulting projection on both the training - and test set after which an LS-SVM with an RBF kernel was tuned and trained. A linear kernel wasn't as performant as the number of dimensions decreased.

kernel outperformed a non-linear one - the number of features is larger and there's not that many data points so a simpler decision boundary may help to avoid overfitting since Cover's theorem implies that it is more likely that the data is linearly separable when the number of dimensions is high (and the number of data points is low).

As some of the features seem less informative than others it may be worthwhile to remove some of them either through PCA or a more sophisticated approach like automatic relevance determination. A basic experiment ended up with the latter selecting 21 features. Training the model on these resulted in an AUC of 0.9973. The results with a larger number of tuning and training runs as well as a comparison with a basic PCA approach are shown in table 2.

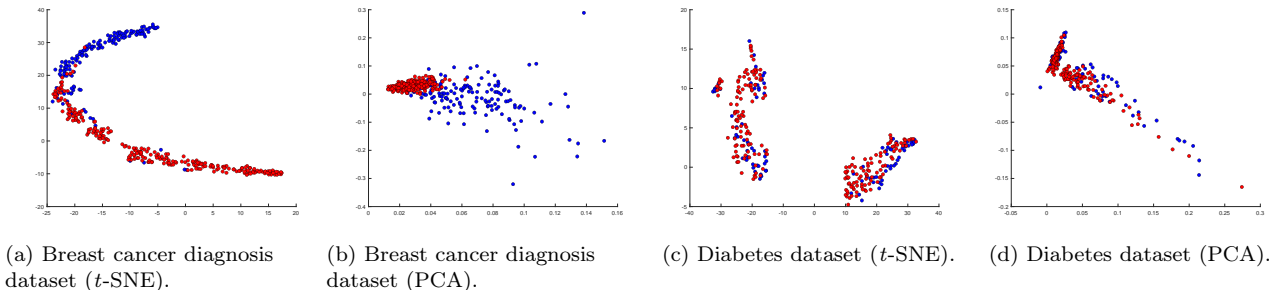


Figure 11: Visualisation of the Wisoncin breast cancer - and the Pima indians diabetes datasets give an idea of how separable they are. The diabetes dataset appears significantly harder and this is reflected in the lower accuracy obtained with various models.

Diabetes dataset

A 2-dimensional visualisation of the 8-dimensional Pima indians dataset (figure 11) reveals it to be more difficult than the previous one (distributions of the input variables tell the same story). Mean error rates of $21.7\% \pm 1.4$, $27.6\% \pm 5.3$ and $22.2\% \pm 1.8$ were obtained with a linear, polynomial and RBF kernel (averaged over 10 runs using tuned parameters)⁵. The average AUCs were 0.844 ± 0.001 , 0.721 ± 0.112 and 0.848 ± 0.004 . An RBF kernel appeared most performant. Automatic relevance determination did not prune any of the input variables which made subsequent poor results with PCA not surprising.

The original paper dealing with this dataset used a custom algorithm related to neural networks. They used all training examples and reached an accuracy of 76%. The performance of an LS-SVM with an RBF kernel trained on the full training set (named `total`) was typically comparable.

While the features may not be informative enough to predict the occurrence of diabetes in this population some further exploration follows.

⁵The AUC for the training set turned out to be quite high for the polynomial kernel (> 0.9) which seemed to imply some degree of overfitting. Changing the cross-validation method to leave-one-out made the AUC for the test set comparable to that of the RBF kernel.

Support vector machine for function estimation

Two datasets are experimented with in figure 12. The first exists of 20 points lying on a slope. Therefore one can expect the linear kernel (which makes for a linear model) to outperform the others. The second (non-linear) dataset is more challenging such that other kernels which enable the SVM to model the non-linearities have to be used instead.

From the problem statement :

$$\min_{w,b,\xi,\xi^*} \frac{1}{2} w \cdot w^T + C \cdot \sum_{k=1}^N \xi + \xi^*$$

where ξ, ξ^* are slack variables representing deviation from the so-called ϵ -insensitive tube it can be deduced that the C (the *bound*) plays the usual role of a regularisation parameter, prioritising either the smoothness of the model or how much it fits the data (i.e. minimising the slack variables). $C = 0$ leads to simple horizontal lines for the linear kernel which express the view that the two input features x_1 and x_2 aren't related. The ϵ parameter controls the width of the tube in which the data points are made to lie. A larger value decreases the number of support vectors and makes the model less accurate.

The formulation resembles that of a least squares fit with Tikhonov regularisation but the ϵ -insensitive tube makes for a different loss function that encourages sparsity and since the problem is turned into a constrained optimisation problem a dual form can be expressed for which one can apply the kernel trick to be able to model any nonlinearities.

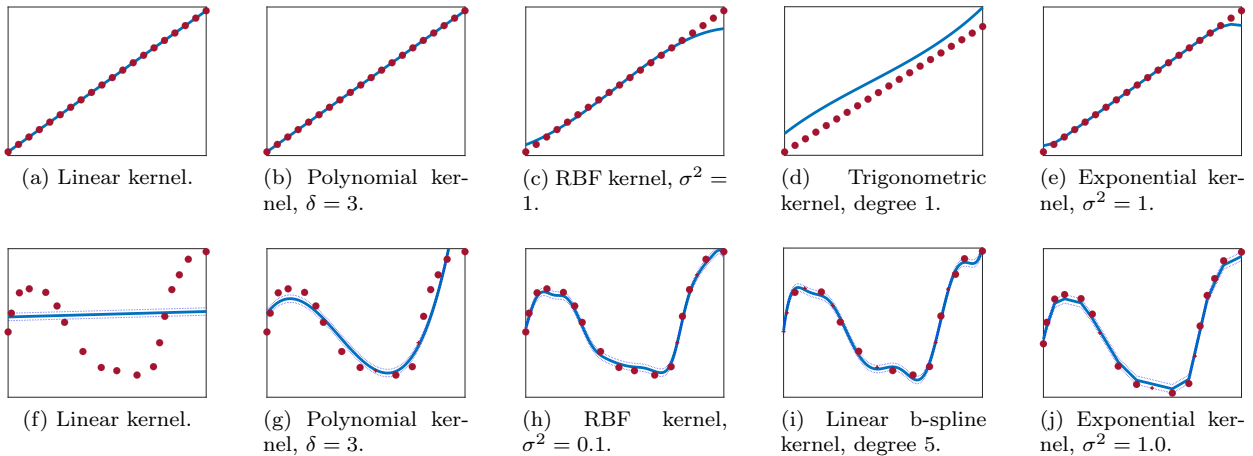


Figure 12: Visualisation of the results of experiments with various kernels and parameters for two different artificial datasets. In the first row $\epsilon = 0$ and `bound` = 10, in the second one $\epsilon = 1$ and `bound` = 1000. Some of the models are likely to be overfitted though these are just toy examples without any test set.

A simple example: the sinc function

Figure 13 shows the results of LS-SVM regression applied on the `sinc` function. The mean squared error is lowest for $\sigma^2 = 1.0, \gamma = 10^6$. The smaller σ^2 value (0.01) leads to overfitting (the noise is being modelled). In this case the underlying function is known and it seems reasonable to take $\sigma \in [0.1, 1.0]$ and, say, $\gamma = 10^3$. However, an optimal parameter cannot be found as it depends on the training set that is being dealt with and even for a given training set there's no unique parameter combination that works best.

Results of automated tuning are shown hereunder :

Method	γ	σ^2	mean squared error
Grid search	$5528319.4668 \pm 54371026.5606$	0.1239 ± 0.1513	0.0104 ± 0.0001
Nelder-Mead	2329.7378 ± 2318.2696	0.1049 ± 0.0892	0.0104 ± 0.0001

Table 3: Results of automated tuning strategies (averaged over 40 runs).

The results are comparable to those obtained previously in the context of classification, with a few outliers for γ . Again, grid search appeared to be slower (185 seconds versus 110 for the simplex method). Some of the models seem to overfit the data a bit.

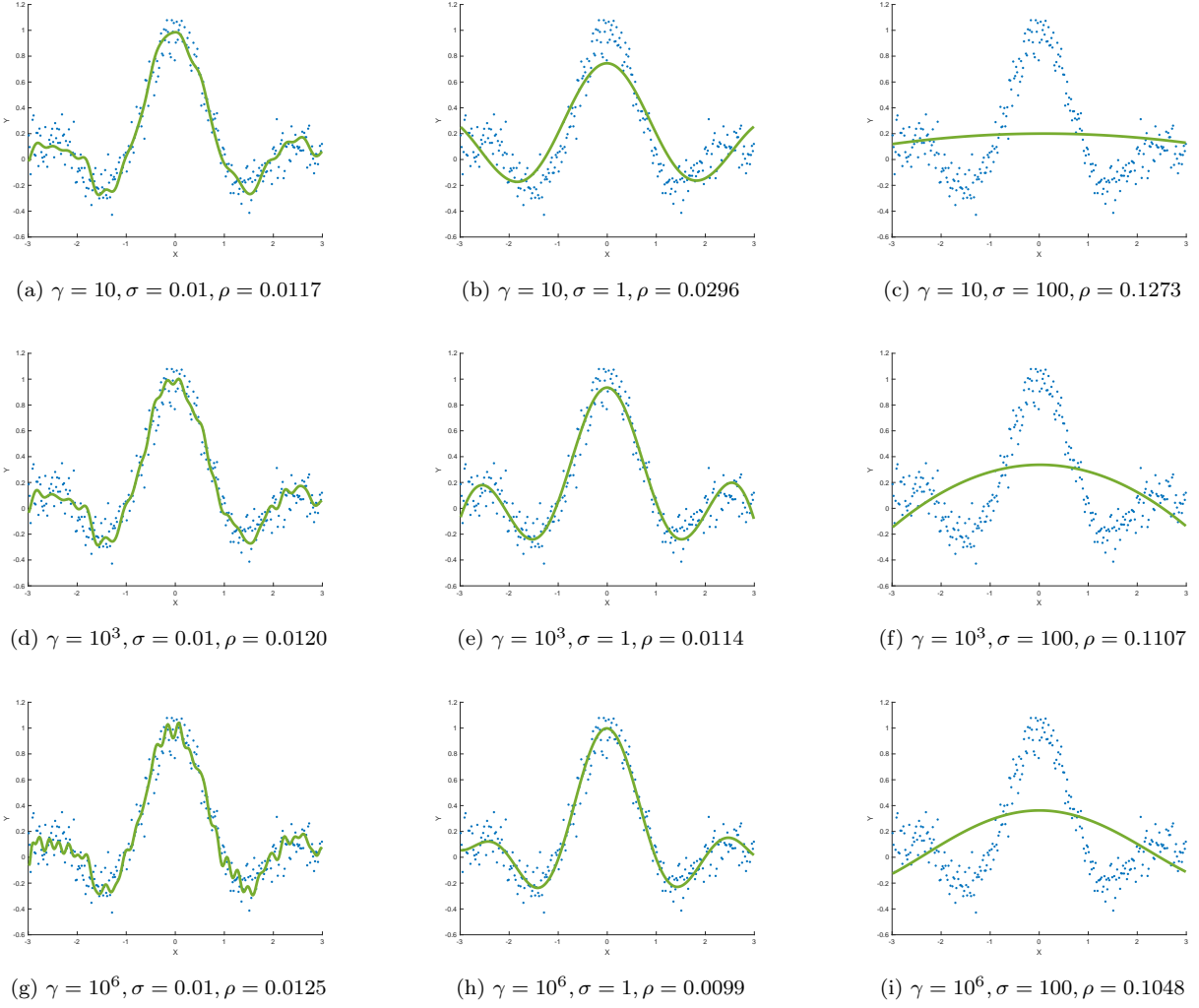


Figure 13: Function estimation experiments with the `sinc` function. Noisy samples are fed to an LS-SVM. The green line is the estimated model, the blue dots represent the test data. ρ is the mean squared error. Small σ values make the model fit the noise.

When making use of a validation set that very set cannot be used for training. Making use of a Bayesian framework is an alternative and allows one to infer appropriate parameter combinations while making full use of the dataset. Depending on the kernel that is being used either 2 or 3 levels of inference are applied. At each of these level Bayes' theorem is used to infer parameter values. The equations are :

$$p(\mathbf{w}, \mathbf{b} | \mathcal{D}, \mu, \zeta_{1_N}, \mathcal{H}_\sigma) = \frac{p(\mathcal{D} | w, b, \mu, \zeta_{1_N}, \mathcal{H}_\sigma)}{p(\mathcal{D} | \mu, \zeta_{1_N}, \mathcal{H}_\sigma)} \cdot p(w, b | \mu, \zeta_{1_N}, \mathcal{H}_\sigma) \quad (1)$$

$$p(\mu, \zeta_{1_N} | \mathcal{D}, \mathcal{H}_\sigma) = \frac{p(\mathcal{D} | \mu, \zeta_{1_N}, \mathcal{H}_\sigma)}{p(\mathcal{D} | \mathcal{H}_\sigma)} \cdot p(\mu, \zeta_{1_N} | \mathcal{H}_\sigma) \quad (2)$$

$$p(\mathcal{H}_\sigma | \mathcal{D}) = \frac{p(\mathcal{D} | \mathcal{H}_\sigma)}{p(D)} \cdot p(\mathcal{H}_\sigma) \quad (3)$$

As indicated by the colourings the evidence at any level equals the likelihood in the next level. At the first level one can take the logarithm of the product to see the relation with the primal form in the LS-SVM problem specification ; while the prior corresponds to the regularisation term the likelihood corresponds to the least squares cost term.

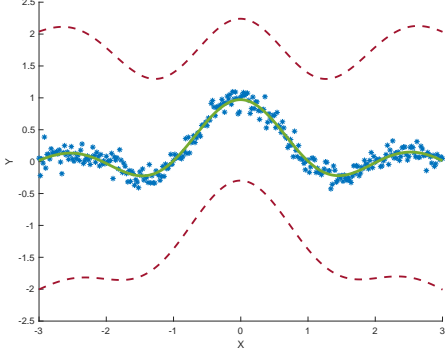


Figure 14: Results of Bayesian inference applied on training data based on the `sinc` function with some added white noise (blue). The function estimate is coloured in green, 95% error bars are indicated in red.

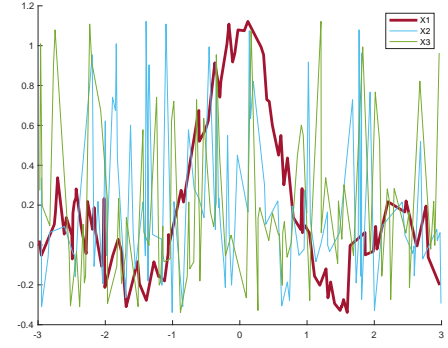


Figure 15: Plot of 3-dimensional input data of which only the first dimension models the `sinc` function, the other 2 being white noise.

One nice facet of this approach is that one ends up with error bars indicating uncertainty of the prediction. These error bars can be seen in figure 14 where the method is applied on the `sinc` function.

Automatic Relevance Determination

By modifying the kernel function for the LS-SVM dual formulation it becomes possible to disregard irrelevant or noisy input dimensions when these don't contribute to the final classification (a form of dimensionality reduction). In the case of an RBF kernel by using a diagonal matrix S as a weighted norm a bandwidth is associated with each of the input dimensions. Level 3 of the Bayesian framework discussed before is then used to infer the elements of S and any input dimensions associated with small bandwidths are iteratively disregarded until no additional improvement is obtained. For the toy dataset the algorithm found x_1 to be the sole relevant one which is also illustrated in figure 15. An other, crude way of doing relevance determination is to consider all possible non-empty subsets of the input features and applying cross-validation on the resulting data to figure out which subset generalises best. For the given data the conclusion remained the same as any subset excluding the first (non-noisy) dimension performed badly ($mse > 0.1$) and the subset excluding all but the first dimensions performed best ($mse \approx 0.012$). This method wouldn't be satisfactory in practice as the power set grows sharply as the number of input dimensions increases. Treating the problem as a global optimisation is more appropriate for example. Or even simply removing random features one by one as long as the results keep on improving.

Robust regression

Two downsides of LS-SVMs are the loss of sparsity and the lack of robustness. Outliers can increase the variance of the decision boundary quite a bit due to the use of the least squares loss, which penalises outliers more than the *mean absolute error* does (such that there is more perturbation). If the noise on the data set is Gaussian then the least squares loss is appropriate, but in general the distribution of the noise is not known and in the case of the toy dataset dealt with here the noise isn't normally distributed. The idea, then, is to find an LS-SVM model as per usual and apply methods from robust statistics on the resulting parameters. Specifically, a weight is assigned to each data point based on its error. Some possible weight functions are shown below.

After assigning the weights a weighted LS-SVM is trained and the whole process may be repeated as desired. Results with 4 weight functions are compared with a non-robust LS-SDM approach in figure 16.

	<i>Huber</i>	<i>Hampel</i>	<i>Logistic</i>	<i>Myriad</i>
<i>Weight function</i> $W(r)$	$\begin{cases} 1 & \text{if } r < \beta \\ \frac{\beta}{ r } & \text{if } r \geq \beta \end{cases}$	$\begin{cases} 1 & \text{if } r < \beta_1 \\ \frac{b_2 - r }{b_2 - b_1} & \text{if } \beta_1 \leq r \leq \beta_2 \\ 0 & \text{if } r > \beta_2 \end{cases}$	$\frac{\tanh(r)}{r}$	$\frac{\delta^2}{\delta^2 + r^2}$

Table 4: Possible weight functions for use in robust regression with LS-SVMs.

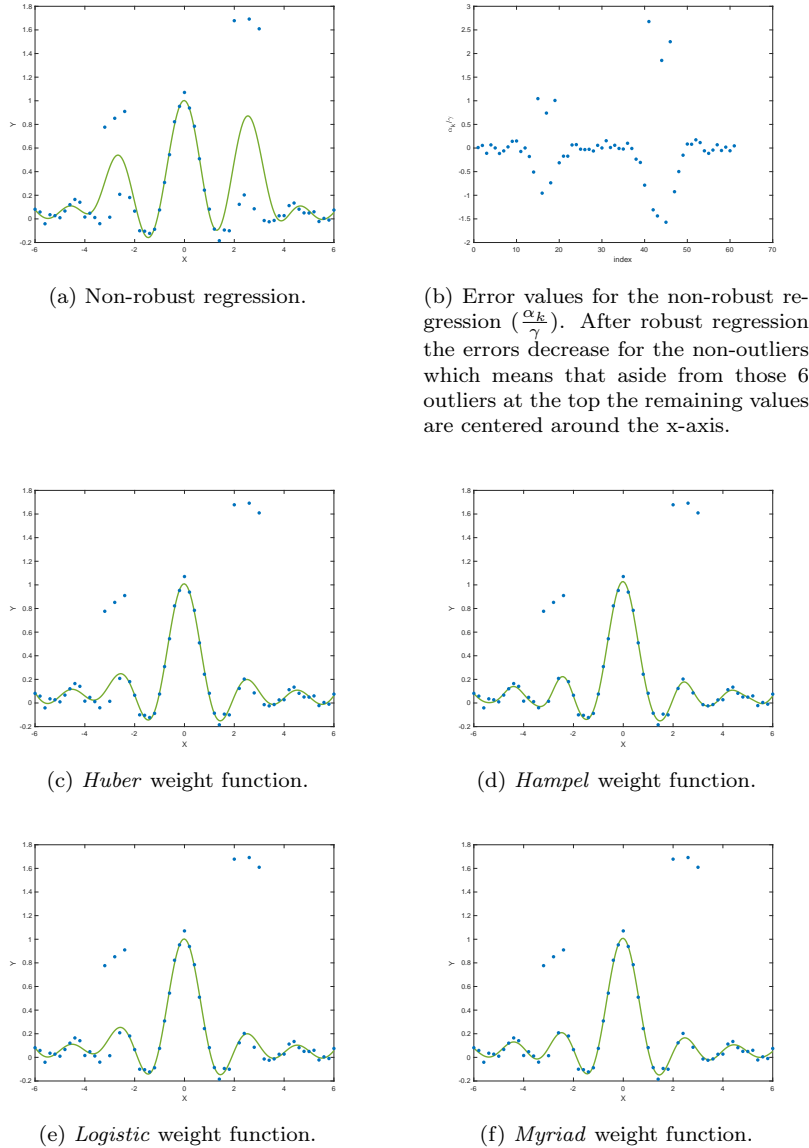


Figure 16: Comparing non-robust regression to robust regression. A variety of weight functions are considered. The smallest mse on the test set was obtained with the *Hampel* weight function. The noise is not normally distributed in contrast with the datasets shown before.

Logmap dataset

The provided model for predicting measurements for the logmap dataset performs quite badly as can be seen below. The results call for the tuning of the three parameters.

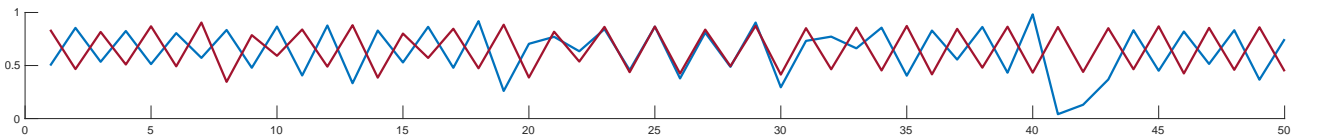


Figure 17: Initial attempt at modelling the logmap dataset (ground truth in blue, prediction in red).

A straightforward way of picking a so-called order of a time series model (i.e. the number of past measurements taken into account for prediction of the next measurement) is to take advantage of the fact that the given dataset is rather small and the order is a discrete variable. This makes it sensible to go over all possible orders and tune regularisation parameter γ and any of the kernel parameters for every possible order separately.

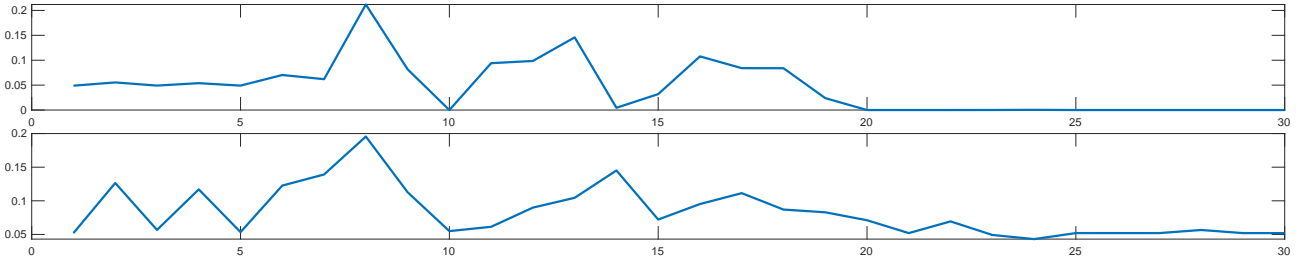


Figure 18: Mean squared errors for just one tuned model per possible order. The top row gives the error for the training set, the bottom row for the test set. A minimum is obtained starting at `order` = 21. The mean absolute errors give a slightly more meaningful picture here because a model predicting the mean value for every time step could have a smaller mean squared error than a more meaningful model (due to the fact that the data lies between 0 and 1).

To find good values for the parameters either cross-validation or the Bayesian framework discussed previously can be used. Both methods were tried and the results with the Bayesian framework are shown in figure 18. In that figure the mean squared errors are plotted in function of the order for LS-SVMs using RBF kernels with tuned parameters. This was measured for the training and the test set. A useful order appeared to lie somewhere in the early 20s and picking anything higher may cause poor generalisation due to overfitting. Results with a model with its order equal to 20 are shown below. The performance has clearly improved.

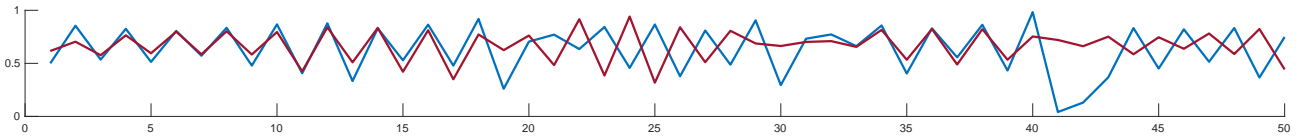


Figure 19: Results for a model using an RBF kernel with tuned parameters. The order is 21, $\gamma \approx 114481.964$ and $\sigma^2 \approx 985.571$.

Santa Fe dataset

The per-order mean squared errors for an analogous tuning approach applied to the Santa Fe dataset (this time by using cross-validation rather than making use of the Bayesian network) are shown in figure 20.

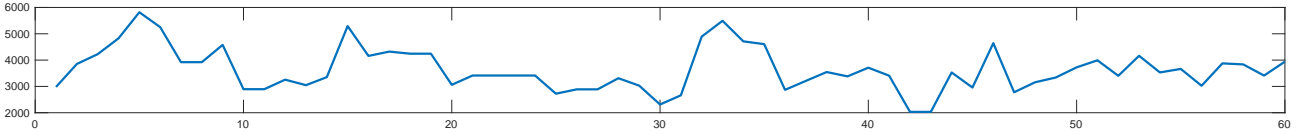


Figure 20: Mean squared errors for various models in function of the order. Parameters were tuned automatically using a grid search. Outliers (large errors) are ‘ignored’ (i.e. set equal to the error for the previous order) to improve the visualisation.

Picking the model with lowest error (prioritising a small order) gave the following result :

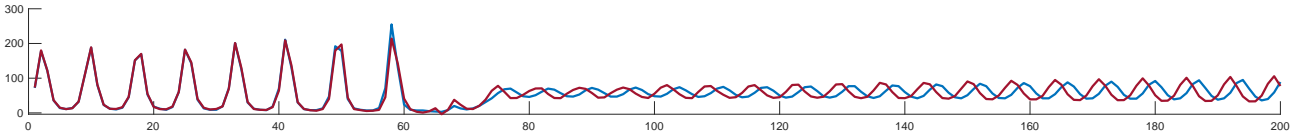


Figure 21: Results for a model using an RBF kernel with tuned parameters. The order is 42, $\gamma \approx 8423.289$ and $\sigma^2 \approx 14.017$.

Due to the limited number of runs the whole tuning procedure by no means proves that this model is best or that this order is optimal. By doing more experiments confidence can grow that certain orders are optimal for this particular dataset.

Up til now only LS-SVMs were toyed with. It’s also possible to work with classical SVMs which - due to the choice of loss function - provide sparsity without necessitating a pruning post-processing step or some other approach to enforce it. The provided MATLAB library has one interesting kernel that is said to perform well for regression, i.e. the ANOVA kernel.

Kernel principal component analysis

The point of *linear principal component analysis (PCA)* is to find a linear transformation (a projection onto an orthogonal basis) such that the variance of the projected data points is maximised. It's an old method introduced by Pearson. The transformed variables are called principal components. By disregarding some of these it is possible to achieve a dimensionality reduction while still capturing most of the important information carried by the input data. This can be used for denoising purposes.

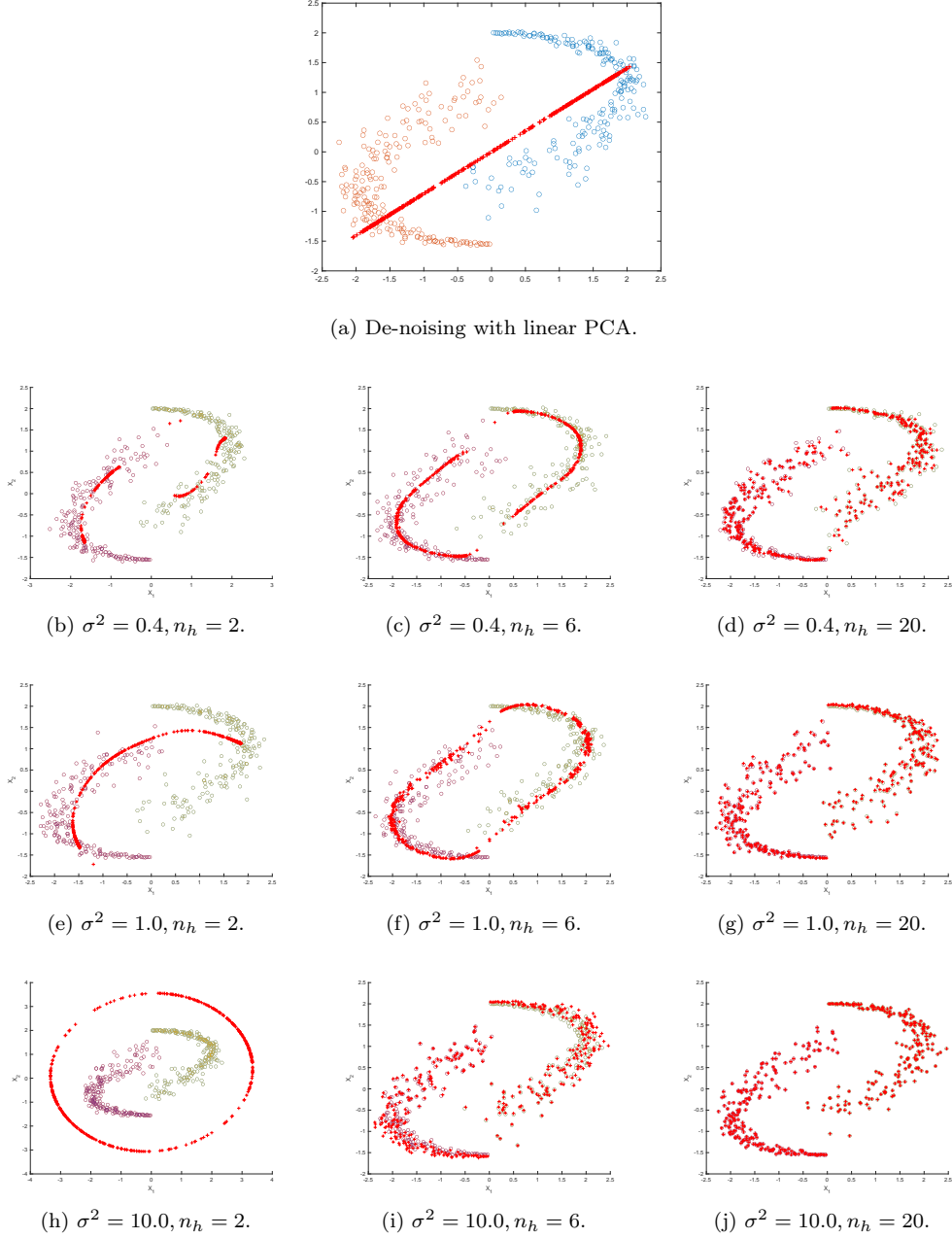


Figure 22: De-noising a toy dataset consisting of two spirals. The number of data points equals 400, the data point dispersion 0.3. n_h is the number of components. All 9 images below the top one use an RBF kernel. De-noising is done by minimising the distance between the feature mapping of an input and its projection in the feature space onto principal axes. Retaining too few principal components leads to a poor result while retaining too many of them prevents any de-noising.

Like *Fisher discriminant analysis (FDA)* it is possible to relate this to LS-SVMs and formulate it as a constraint optimisation problem :

$$\max_{w,e} \quad \mathcal{J}_P(w, e) = \gamma \frac{1}{2} \sum_{k=1}^N e_k^2 - \frac{1}{2} w^T w \quad \text{such that } e_k = w^T \cdot x_k \quad (k = 1, \dots, N)$$

The errors represent the variance after projection which is to be maximised. Here too, a dual form can be introduced using Lagrange multipliers. This makes it possible to apply the kernel trick which can make for a non-linear approach (in which case PCA is applied in the feature space). Additionally an increase in the number of dimensions becomes possible when the number of training samples is larger than the number of dimensions. The bias term is responsible for centering the kernel matrix automatically rather than having to do this beforehand. This is especially interesting in the case of *kernel spectral clustering (KSC)* which is considered in the next paragraph and where centring is not a straightforward thing to do.

Because the alternative PCA formulation is model-based it becomes possible to do so-called out-of-sample extensions - the solution is not limited to the input data. It also becomes possible to tune models and find the right parameters that fit the data. However, because of the unsupervised nature of PCA this is not trivial. If the resulting model is meant to be used as a sort of preprocessing step e.g. for use in classification or in the context of a reconstruction problem (assuming an information bottleneck) then tuning can be done on the basis of the related loss function by making use of validation sets (as demonstrated previously). Otherwise it is possible to apply cross-validation techniques based on pre-images to find useful values of the kernel parameters. These pre-images are approximations of inverse transformations of kernel PCA outputs back to the input space and can be used to calculate the reconstruction error for any point in the validation set (which consists of one data point in the case of LOOCV). They can be determined for any input vector x by finding the input vector z which minimises $\|\phi(z) - P_{n_c} \cdot \phi(x)\|^2$ (where $\phi(x)$ is the feature mapping of input z and $P_{n_c} \cdot \phi(x)$ is the projection of x onto a subspace in the feature space spanned by the n_c first eigenvectors found through kPCA).

More appropriate (less costly) approaches to tune the parameters include kernel Parallel Analysis (kPA) which is an extension of classical Parallel Analysis (PA). PA is used to find out an appropriate number of components for PCA instead of just going by manual inspection of the scree plot or applying a rule like Kaiser's (taking all eigenvectors for which the eigenvalue is larger than 1). Also possible is Model selection based on Distance Distributions (MDD) which improves upon kPA by improving noise estimation when the number of dimensions is low.

Consider the de-noising of a toy dataset for which the resulting pre-images after kernel PCA using various parameter values are shown in figure 22. Tuning is done manually. When the number of principal components increases the reconstruction improves which is not surprising. More meaningfully, retaining a smaller number of principal components results in good de-noising performance. As per usual the linear approach (classical PCA) is not able to capture the non-linearities in the input data leading to poor results for this particular dataset. The σ^2 parameter in the Gaussian kernel can lead to a loss of non-noisy information when set too low (or a lack of de-noising if set too high, as seen in figure 22).

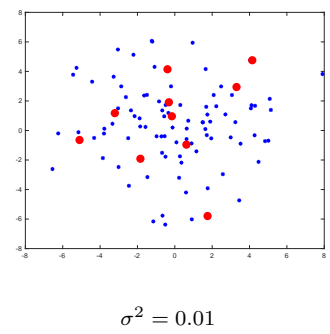
Spectral clustering

Classification problems were considered in the first section of this report. In a classification setting a model is constructed which is made to predict what class some data point belongs to. These models are trained in a supervised way i.e. there's an annotated training set and test set which are used to determine appropriate parameters for the model and for evaluating it. In a clustering setting the number of classes k is not necessarily set beforehand but can be tuned. A model is trained in an unsupervised manner such that it clusters data points on the basis of some similarity measure.

Spectral clustering in particular deals with finding a minimal cut of a similarity graph (a weighted & undirected graph) rather than finding a decision boundary which separates classes. Since finding a balanced yet minimal cut is NP-hard a relaxed version is considered instead. The solution of the relaxed version is based on the eigendecomposition of the Laplacian matrix of the graph such that the data points can be embedded in an eigenspace on which a clustering algorithm like *k-means* can be applied.

The Laplacian matrix captures a lot of information about the graph such as the number of connected components (which equals the multiplicity of the eigenvalue $\lambda = 0$). Related to this number is the property that if the data is sorted according to cluster membership the similarity matrix becomes block-diagonal. Such depictions are used in the figures above.

Kernel spectral clustering (KSC) reformulates spectral clustering as an LS-SVM, essentially boiling down to a weighted version of kernel PCA. Again, out-of-sample extensions become possible and one can apply it on large-scale



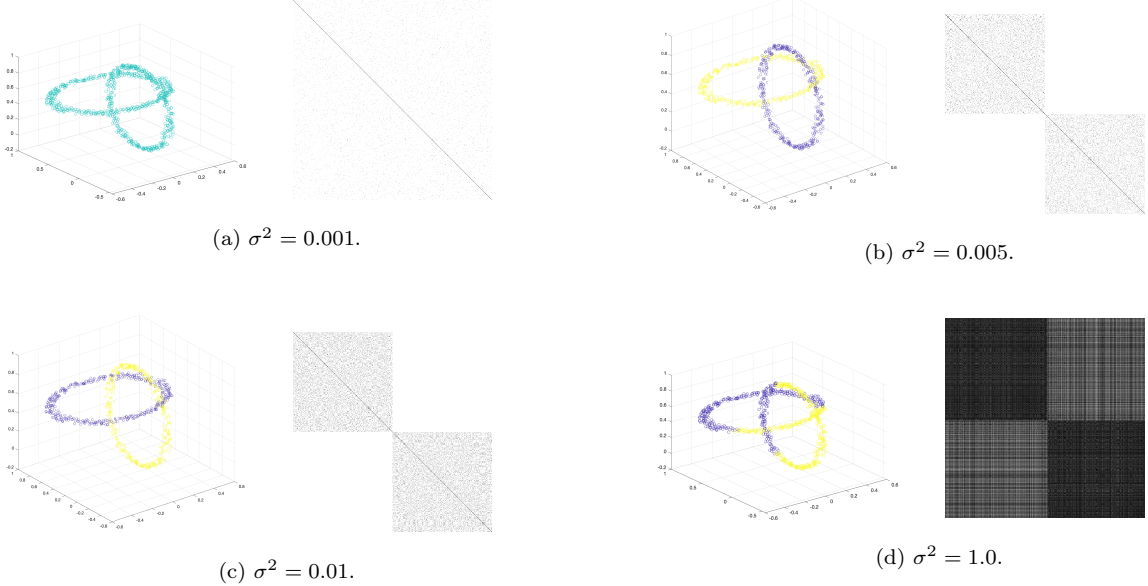


Figure 23: Clustering of a toy dataset consisting of two rings. KSC applied using a kernel with varying σ^2 values. When this bandwidth is too large the reach of influence of each data point becomes too large and the clustering becomes subpar.

problems.

Experiments with an RBF kernel are shown in figure 23. Since the similarity matrix is the Kernel function and σ^2 happens to control the contrast in similarity between data points a σ^2 value which is small leads to a single class as all points are considered similar while a larger σ^2 leads to poor clustering results.

Fixed-size LS-SVM

Sometimes the amount of data that is being dealt with is too large such that some of the matrices like the kernel matrix involved in the dual formulations cannot be stored in memory. It becomes desirable, then, to solve the problem in the primal rather than in the dual space (it's the other way round when the number of input dimensions is high). The problem with this is that the feature map $\phi(x)$ is generally not known, only the kernel function representing dot products is made explicit.

While decomposition can be used for this an approach that can be considered in the case of fixed-size LS-SVMs is the Nyström method which is traditionally used for integral approximation. In the current setting it means that one takes a random subsample of the input data (of size $M \ll N$) and then uses this to approximate the feature map $\phi(x)$ such that a parametric solution can be found. For fixed-size LS-SVMs the subsample starts randomly and is then updated iteratively as long as the Renyi entropy improves. This metric can be approximated by taking the sum of the elements of the kernel.

Examples of subsamples obtained through optimisation of the Renyi entropy are shown in figure 24. The kernel is a Gaussian one, the input data is normally distributed. It looks as though a larger value for σ^2 leads to a selection of data points that are more spread out.

In figure 25 a fixed-size LS-SVM approach is compared with a variant which applies an ℓ_0 -penalty after generating a fixed-size LS-SVM solution. This post-processing does not influence the total runtime because its complexity is $\mathcal{O}(M^3)$ while that of the fixed-size LS-SVM is $\mathcal{O}(NM^2)$. While the error

increases the number of support vector is much lower for the latter method. This is not surprising since the ℓ_0 -norm counts the number of non-zero values which means that it aims for sparse representations. The error drops as well, presumably because the model generalises better.

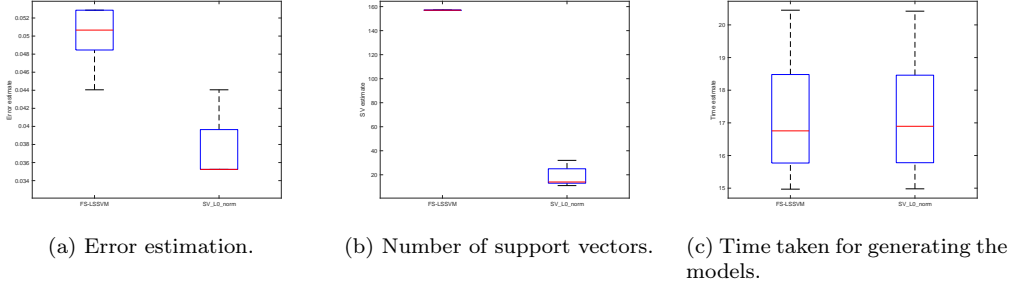


Figure 25: Comparison of the standard fixed-size LS-SVM approach with a modified approach applying an ℓ_0 -penalty to obtain a sparser representation.

Kernel principal component analysis

De-noising a quite noisy USPS dataset with classical PCA gives poor results at best (see figure 26). Kernel PCA with an RBF kernel manages to exploit the data much more and the results are a big improvement (see figure 27).

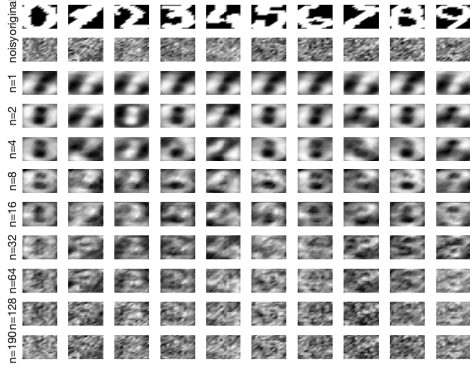


Figure 26: Results of linear PCA applied to the USPS dataset (top rows are original and noisy data, next 9 rows are results for $n_c \in [1, 2, 4, 8, 16, 32, 64, 128, 190]$).

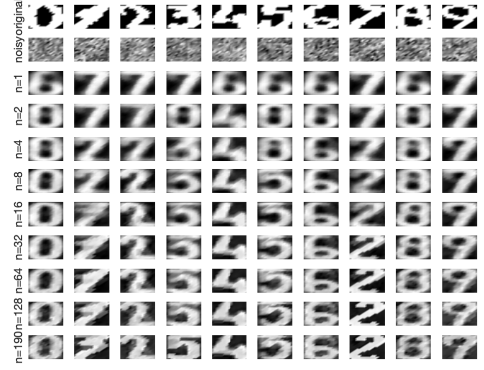


Figure 27: Results of kernel PCA applied to the USPS dataset (top rows are original and noisy data, next 9 rows are results for $n_c \in [1, 2, 4, 8, 16, 32, 64, 128, 190]$).

What was noted in the yin-yang toy dataset shown at the beginning of this section can be observed again in figure 28 ; small bandwidths remove important information (such that some digits get reconstructed without noise but as the wrong number) while larger ones fail to de-noise and noise is re-introduced slowly but surely in the reconstructions. In the first section of this report large bandwidths reduced the solution to something equivalent to a simple linear classifier, for the USPS dataset the same thing happens where large bandwidths make the results resemble that of classical, linear PCA.

The small bandwidths cause the data points to be considered highly dissimilar and only the very strong directions of variation are extracted which makes for virtually noise-free yet completely wrong reconstructions. Conversely, very high bandwidths cause the data points to be considered very similar to each other and it gets harder to find meaningful directions of variation such that the noise is considered informative again.

It was stated previously that one way to tune kPCA is to measure reconstruction errors for the validation set to gauge the effectiveness of certain parameter combinations. A plot of the reconstruction errors measured for the provided training and validation sets is provided in figure 29. The errors tell a meaningful story which also corresponds with the visualisation of the performance of various parameter combinations in figure 28.

Fixed-size LS-SVM

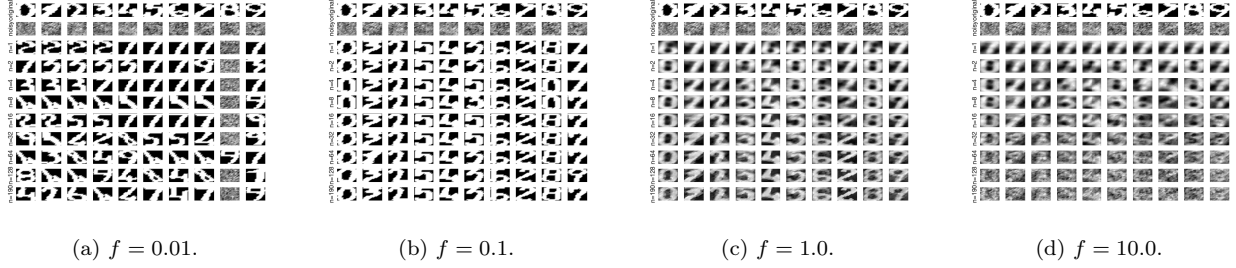


Figure 28: De-noising the USPS hand-written digit dataset. f is a factor with which is multiplied by about 51 to get the bandwidth.

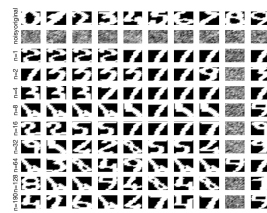


Figure 29: Reconstruction error for the training and validation sets in function of the bandwidth.